

Indenofluorene-Based Blue Fluorescent Compounds and Their Application in Highly Efficient Organic Light-Emitting Diodes

Kum Hee Lee,^[a] Seul Ong Kim,^[a] Sunwoo Kang,^[a] Jin Yong Lee,^[a] Kyoung Soo Yook,^[b] Jun Yeob Lee,^{*[b]} and Seung Soo Yoon^{*[a]}

Keywords: Photophysics / Luminescence / Organic light-emitting diodes / Fused-ring systems

Blue fluorescent compounds based on indenofluorene derivatives incorporating the (diphenylamino)arylvinyl group and di-*tert*-butylphenyl blocking units have been synthesized by Suzuki coupling and the Horner–Wadsworth–Emmons reaction. Their electroluminescence in multilayered OLEDs was examined; the devices have the structures ITO/DNTPD/NPB/MADN:blue dopant/Alq3/LiF/Al. A device with 7% 2-(3,5-di-*tert*-butylphenyl)-8-(9,9-diethyl-2-(diphenylamino)-fluorene-7-yl-ethenyl)-6,6,12,12-tetraethylindeno[1,2-*b*]fluorene (**3**) as blue dopant showed a luminous efficiency of

12.2 cd A⁻¹, a power efficiency of 6.08 lm W⁻¹, and an external quantum efficiency of 7.84% at 20 mA cm⁻² with CIE (Commission Internationale d'Éclairage) (x, y) coordinates of (0.148, 0.241) at 8.5 V. A deep-blue OLED with CIE (x, y) coordinates of (0.153, 0.128) doped with 2-(3,5-di-*tert*-butylphenyl)-8-[9-(3,5-di-*tert*-butylphenyl)carbazol-3-yl-ethenyl]-6,6,12,12-tetraethylindeno[1,2-*b*]fluorene (**4**) exhibited a luminous efficiency of 3.25 cd A⁻¹, a power efficiency of 1.74 lm W⁻¹, and an external quantum efficiency of 2.93% at 20 mA cm⁻².

Introduction

Conjugated polycyclic aromatic compounds have optical and electronic properties suitable for photonic and electronic devices such as organic light-emitting diodes (OLEDs).^[1–4] Fluorene derivatives are particularly attractive light-emitting compounds for OLEDs due to their high photoluminescence (PL) efficiency, wide bandgap, good solubility, and excellent thermal and chemical stabilities.^[5–10] Because the optical, chemical, and electronic characteristics of fluorene arise from its rigid and planar biphenyl moiety, structurally related indenofluorene, with a planar and longer conjugated *p*-terphenyl moiety, is also a promising compound. Blue compounds containing indenofluorene backbones instead of fluorene units have led to enhanced OLED properties.^[11–15] However, fluorescent molecules based on indenofluorene can form aggregations or excimers leading to an unwanted long-wavelength emission band and decreased luminescent efficiency. The energy bandgap of an indenofluorene core is also too large to be suitable for use in blue organic light-emitting diodes. These problems are mainly solved by the introduction of sterically bulky sub-

stituents and moieties to control the HOMO and LUMO energies of the indenofluorene core. Indenofluorenes have unique geometries that allow the methylene bridges to be either on the opposite side (indeno[1,2-*b*]fluorene) or on the same side (indeno[2,1-*b*]fluorene) of the terphenyl core. Although the electrochemical and photophysical properties of indenofluorenes have been studied, the dependence of electroluminescent properties on positional isomerism has not yet been reported.^[16]

In this paper we report the synthesis and electroluminescent (EL) properties of a new series of indenofluorene derivatives **1–5** with various aromatic groups at the terminal 2- and 8-positions. The indeno[1,2-*b*]fluorene derivatives **1–4** have two methylene moieties at the C-6 and C-12 positions each alkylated with two ethyl groups. They have non-coplanar structures, which effectively inhibits molecular aggregation and excimer formation in the solid state. The incorporation of a bulky di-*tert*-butylphenyl group at the 8-position could improve solubility and prevent molecular aggregation and self-quenching. The attachment of electron-rich groups such as (diphenylamino)phenylvinyl, (diphenylamino)biphenylvinyl, (diphenylamino)fluorenylvinyl, and di-*tert*-butylphenylcarbazolylvinyl at the 2-position of the indenofluorene core can control the energy bandgaps of the dopants by increasing the HOMO energies, which could make the compounds suitable for use as blue emitters in OLEDs. These groups also enhance the hole transport properties of **1–5** and thus lead to improved OLED efficiency and stability. Compound **5**, an isomer of compound **1**, was designed to study the effects of structural changes in the core of indenofluorene derivatives on the EL perform-

[a] Department of Chemistry, Sungkyunkwan University, 300 Cheoncheon-dong, Jangan-gu, Suwon, Gyeonggi, 440-746 Korea

Fax: +82-31-290-7075

E-mail: syyoon@skku.edu

[b] Department of Polymer Science and Engineering, Dankook University,

126, Jukjeon-dong, Suji-gu, Yongin, Gyeonggi, 448-701 Korea

Supporting information for this article is available on the WWW under <http://dx.doi.org/10.1002/ejoc.201200117>.

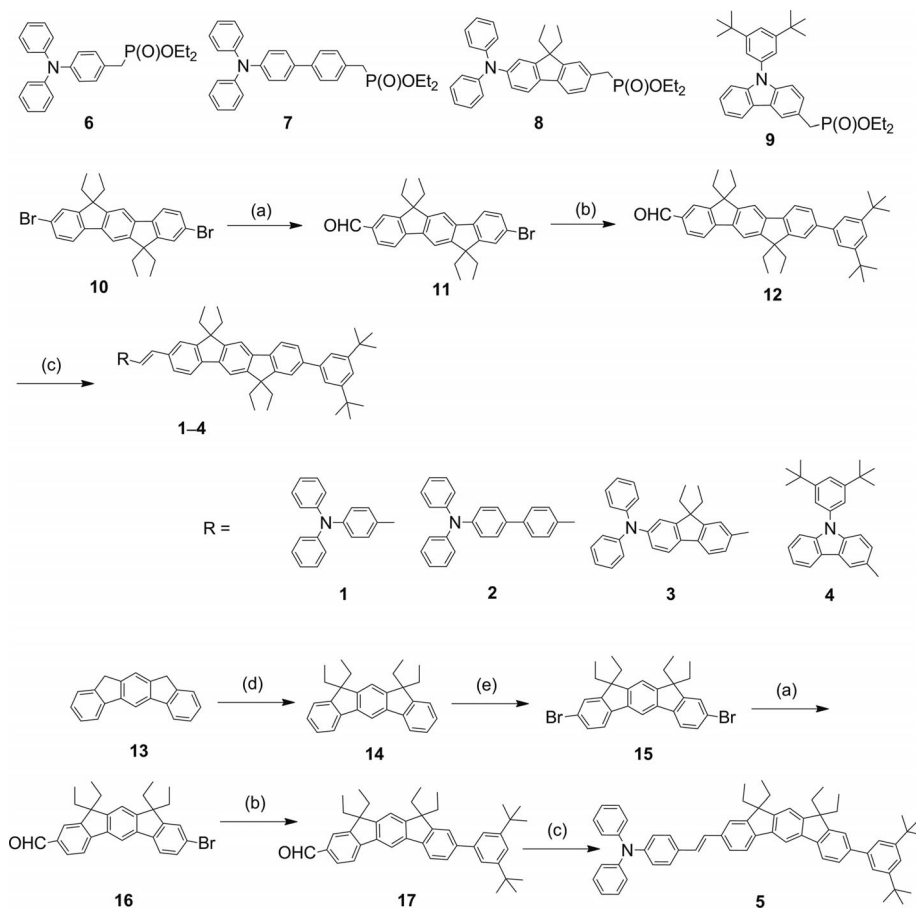
ance of devices. Herein, highly efficient blue OLEDs have been demonstrated that incorporate these indenofluorene-based blue emitters as dopants.

Results and Discussion

The indenofluorene derivatives **1–5** were synthesized as outlined in Scheme 1. Compound **10** was synthesized by an established procedure^[15,17] involving a Suzuki coupling reaction, oxidation, Wolff–Kishner reduction, alkylation, and bromination. It was monolithiated by using a stoichiometric amount of *n*BuLi in a lithium/halogen exchange reaction at $-78\text{ }^{\circ}\text{C}$, followed by reaction with DMF to afford the monoformylated **11**. The intermediate **12** was produced by the Suzuki cross-coupling reaction of monoformylated **11** and 3,5-di-*tert*-butylphenylboronic acid in aqueous solution. Finally, the blue light-emitting compounds **1–4** were produced in moderate yields (48–57%) by Horner–Wadsworth–Emmons reactions between the corresponding phosphonates and intermediate **12**. Compound **5**, a positional isomer of compound **1**, was produced similarly to compound **1**, starting from 1,3-dihydroindeno[2,1-*b*]fluorene (**13**).^[18] It was produced in 81% yield. The molecular structures of all the compounds were characterized by ^1H

and ^{13}C NMR, FTIR, and low- and high-resolution mass spectroscopy. High-pressure liquid chromatography showed that the compounds were all prepared with a purity of at least 99.0%.

Figure 1 shows the UV/Vis absorption and PL spectra of the blue dopant compounds in dilute CH_2Cl_2 solutions and as thin films formed on quartz plates. Table 1 summarizes their optical and photoluminescent properties. Figure 1 (a) shows that the absorption spectrum of compound **2** is blue-shifted by around 6 nm relative to the normalized optical absorption spectra of compound **1** as a result of distorted π conjugation at the inner biphenyl unit, which reduces the length of the π conjugation of **2** relative to **1**. Compound **3** shows a spectrum redshifted by around 4 nm relative to compound **1** due to increased π conjugation at the inner fluorene unit. Compound **4** shows a 10 nm hypsochromic shift relative to compound **1** due to differences in the electronic properties of the triphenylamine and phenylcarbazole units. The spectrum of **5** exhibits an absorption band hypsochromically shifted by 51 nm relative to **1**, which corroborates previous observations on the indeno[1,2-*b*]fluorene and indeno[2,1-*b*]fluorene cores.^[16] Compared with the indeno[1,2-*b*]fluorene core, π conjugation in indeno[2,1-*b*]fluorene is ineffective due to the unfavorable or-



Scheme 1. Synthesis of compounds **1–17**. Reagents: (a) *n*BuLi, DMF, THF; (b) 3,5-*(t*Bu)₂C₆H₃B(OH)₂, [Pd(PPh₃)₄], 2 M Na₂CO₃, ethanol, toluene; (c) RCH₂PO(OEt)₂, *t*BuOK, THF; (d) *n*BuLi, bromoethane, THF; (e) Br₂, FeCl₃, CHCl₃. See the Exp. Section for full details.

bit interaction between the *meta* position of its central benzene ring, which would lead to a shorter π -conjugation length in **5** than in **1**. Figure 1 (a) shows overlapping between the absorptions of the five blue dopants and the emission of the common host compound 2-methyl-9,10-bis(2-naphthyl)anthracene (MADN). Overlapping of the emission of MADN with the absorption spectra of the dopants decreased as follows: **3** > **1** > **2** > **4** > **5**. Energy-transfer

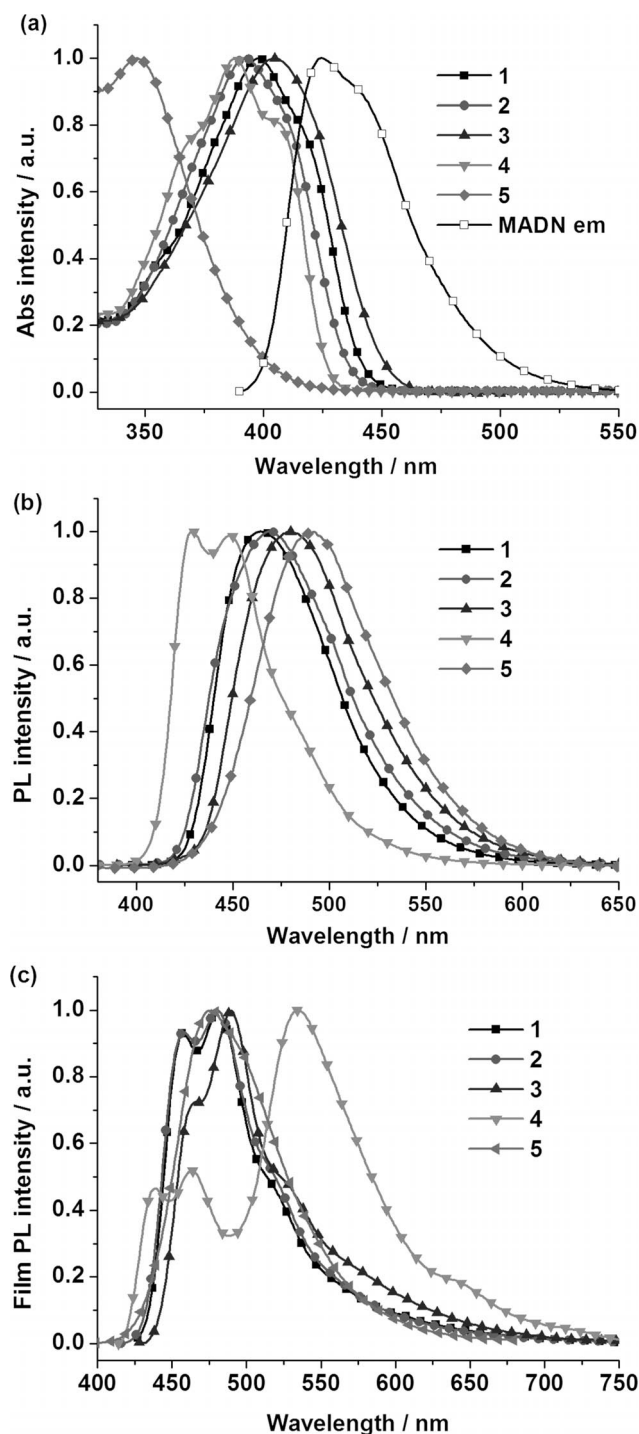


Figure 1. (a) UV absorption and (b) PL spectra of compounds **1–5** and emission spectra of the common host MADN in dilute CH_2Cl_2 solution. (c) PL spectra of compounds **1–5** as thin films.

efficiency is highly dependent on the spectral overlap between the emission of the host and the absorption of the dopant. Therefore all five blue compounds could effectively accept energy from the MADN host by Förster energy transfer, with the efficiencies of energy transfer ranked similarly to the extent of the overlap. Part b of Figure 1 shows the blue fluorescence of the compounds **1–5** to have maximum emission wavelengths at 464, 469, 480, 429, and 492 nm, respectively. The band-gap energies range from 2.80 to 2.97 eV, narrower than the 3.0 eV exhibited by the MADN host. The PL spectrum of **3** is redshifted relative to that of **1**, which suggests that its larger π -conjugated fluorene group reduces the HOMO–LUMO energy gap. The distorted structure of compound **2** leads to breaks in the conjugation along the framework and thus localization of the π electrons, increasing its energy gap relative to compound **3**. Compound **4**, which contains a carbazole unit, shows a hypsochromic shift relative to compounds **1–3**, which contain triphenylamine, (diphenylamino)biphenyl, and (diphenylamino)fluorene units, respectively. These results indicate that the carbazole moiety of the indeno-fluorene derivative increases the bandgap energy. Interestingly, compound **5**, with an indeno[2,1-*b*]fluorene core, exhibits absorption at a shorter wavelength but has a much longer emission wavelength than compound **1** with an indeno[1,2-*b*]fluorene core. This implies that the properties of the excited states of compound **5** are very different to those of compound **1**. The fluorescent emission quantum yields were determined by using BDAVBi ($\Phi = 0.86$ in CH_2Cl_2) as a standard and they decrease as follows: **3** (0.97) > **1** (0.79) > **4** (0.71) > **2** (0.46) > **5** (0.25). Compound **1** exhibits a fluorescent emission quantum yield 3.20 times that of **5**, which indicates that the indeno[1,2-*b*]fluorene core improves the emission quantum yield more than the indeno[2,1-*b*]fluorene core.

The HOMO energies of the dopants were estimated by using an AC-2 photoelectron spectrometer; the LUMO levels were calculated by subtracting the corresponding optical bandgap energies from the HOMO values. The HOMO energies of compounds **1–5** were estimated to be -5.34 , -5.62 , -5.48 , -5.29 , and -5.54 eV, respectively, and their LUMO energies were calculated to be -2.49 , -2.73 , -2.68 , -2.32 , and -2.61 eV, respectively. Figure 2 shows the HOMO and LUMO energies of the blue fluorescent compounds along with those of other compounds used in EL devices: indium tin oxide (ITO), *N,N'*-diphenyl-*N,N'*-bis[4-(phenyl-*m*-tolylamino)phenyl]biphenyl-4,4'-diamine (DNTPD), *N,N'*-bis(1-naphthyl)-*N,N'*-diphenylbenzidine (NPB), MADN, tris(8-hydroxyquinolinyl)aluminium (Alq_3), and LiF/Al.

To explore the observed photophysical properties of the organic lighting-emitting diode compounds, density functional theory calculations were carried out by using the B3LYP hybrid functional with the 6-31G* basis set by using the Gaussian 03 suite of programs.^[19] The distributions of the HOMOs and LUMOs are shown in Figure 3. The dihedral angles between the phenyl (carbazole/fluorene) and indenofluorene moieties were calculated to be 16.15, 1.89,

Table 1. Photophysical data for compounds 1–5.

	λ_{abs} [nm] ^[a]	λ_{em} [nm] ^[a,b]	FWHM [nm] ^[a,b]	Φ_{F} ^[c]	$\Phi_{\text{F}}(\text{film})$ [%] ^[d]	ΔE [eV] ^[e]	LUMO/HOMO [eV] ^[f]
1	398	464/481	66/70	0.79	10	2.85	−2.49/−5.34
2	392	469/480	75/76	0.46	16	2.89	−2.73/−5.62
3	402	480/490	73/71	0.97	15	2.80	−2.68/−5.48
4	388	429,448/463,534	58/129	0.71	12	2.97	−2.32/−5.29
5	347	492/477	73/77	0.25	99	2.93	−2.61/−5.54

[a] Measured in CH_2Cl_2 solution. [b] Measured in film. [c] Values of Φ_{F} were determined in CH_2Cl_2 solution at 298 K against BDAVBi as reference ($\Phi = 0.86$). [d] The fluorescent quantum yields of thin films were determined by using BDAVBi film as standard ($\Phi_{\text{F}} = 30\%$ measured by the calibrated integration sphere system). [e] ΔE is the bandgap energy estimated from the intersection of the absorption and photoluminescence spectra. [f] The HOMO energies were determined by using a low-energy photoelectron spectrometer (Riken-Keiki, AC-2) and LUMO = HOMO + ΔE .

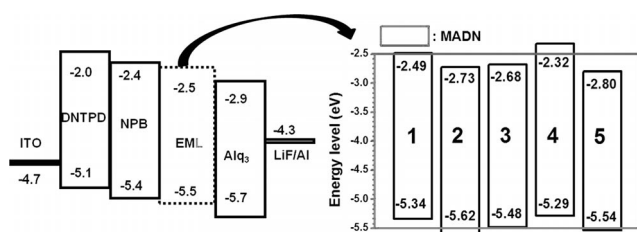


Figure 2. Energy-level diagram for compounds 1–5 used in OLED fabrication.

15.34, 16.62, and 10.21°, respectively. The HOMO electrons are distributed over the (diphenylamino)phenyl(fluorenyl)-vinylindenofluorene moiety in **1**, **3**, and **5**, whereas in the LUMO, the electrons are distributed over the phenyl(fluorenyl)vinylindenofluorene moiety. The HOMO of **2** has electrons distributed over the (diphenylamino)biphenylvinylindenofluorene moiety, whereas the electrons in the LUMO are distributed over the biphenylvinylindenofluorene. Compound **4** has electrons distributed over the cabazolyvinylindenofluorene moiety in the HOMO and over the vinylindenofluorene moiety in the LUMO.

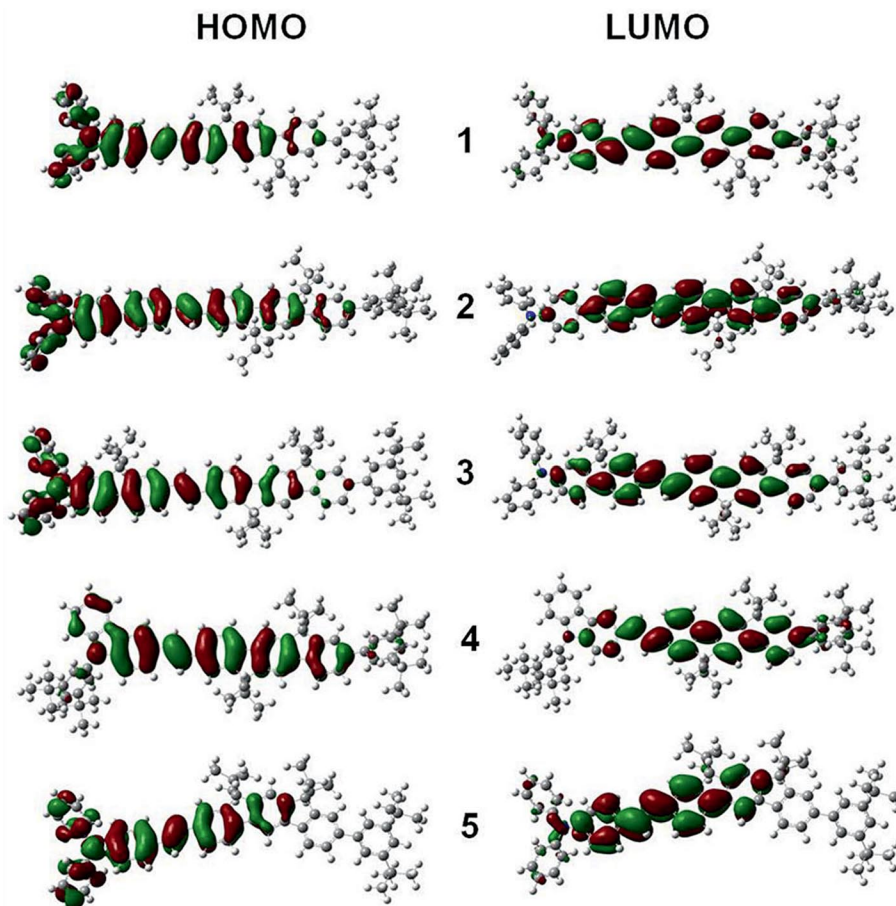


Figure 3. HOMOs and LUMOs of 1–5 calculated at the B3LYP/6-31G* level of theory.

The electronic transition properties of compounds **1–5** were investigated by time-dependent DFT (TDDFT) calculations carried out on the DFT-optimized geometries. Only HOMO-to-LUMO transitions contributed to the electronic transitions in all the compounds. The HOMO energies of **1–5** lie within a narrow range, as do their LUMO energies. The excitation energy of **1** was calculated to be 2.8311 eV, which corresponds to an absorption wavelength of 437.94 nm. The excitation energies of **2** and **3** were calculated to be 2.8225 and 2.7435 eV, respectively, which correspond to longer absorption wavelengths than those shown by **1**, 439.27 and 451.91 nm, respectively. This difference is due to the lengths of the chromophores. The HOMOs of **2** and **3** show better delocalized electron density than that of **1** (Figure 3). The excitation energy of **4** was calculated to be 2.9751 eV (416.74 nm), which is slightly redshifted relative to that of **1**. This is due to the HOMO in **1** showing greater delocalized electron density than that of **4**. The carbazole moiety appears to destabilize the HOMO and LUMO more than the diphenylamine moiety. The excitation energy of **5** was calculated to be 2.9549 eV, corresponding to an absorption wavelength of 419.51 nm, which is hypsochromically shifted relative to that of **1**. This is due to **5** having a more planar structure than **1**, which leads to increased delocalization of the electron density. These results are in good agreement with the experimentally observed absorption wavelengths.

The electroluminescent properties of **1–5** were examined by testing devices fabricated by thermal deposition with configurations of ITO/DNTPD (60 nm)/NPB (30 nm)/dopant (*x*%):MADN host (30 nm)/Alq₃ (20 nm)/LiF (1.0 nm)/Al (200 nm). DNTPD acts as a hole-injection layer, NPB as a hole-transporting layer, MADN as host, and Alq₃ as an electron-transporting layer. The electroluminescent properties of **1–5** were optimized by testing host/dopant emitting systems incorporating **1–5** as blue dopants at concentrations of 3, 5, and 7% with MADN as the common fluorescent host.

With a doping concentration of 7%, devices **1C–5C**, doped with **1–5**, respectively, exhibited blue emission at 8.5 V with Commission Internationale d'Éclairage (CIE) coordinates of (0.146, 0.212), (0.149, 0.193), (0.151, 0.257), (0.153, 0.128), and (0.216, 0.355), respectively [Figure 4 (a)]. Device **2C**, the dopant of which contains a biphenyl spacer group, shows blueshifted CIE coordinates relative to **1C**, those of **3C**, the dopant of which contains a fluorenyl spacer group, are redshifted, **4C**, the dopant of which contains a di-*tert*-butylphenylcarbazolylvinyl group rather than a (diphenylamino)arylvinyl group (**1–3**), shows blueshifted CIE coordinates due to the electronic effects of the *tert*-butylated carbazole moiety. Device **5C**, which contains the dopant with the indeno[2,1-*b*]fluorene core, shows significantly redshifted CIE coordinates relative to the device **1C**, which contains the indeno[1,2-*b*]fluorene core, in good agreement with the PL spectra of the corresponding dopants. Normalized EL spectra of devices **4A–C**, which are fabricated with dopant **4** at concentrations of 3, 5, and 7%, respectively, show stable blue EL with little variation in the

CIE coordinates with doping concentration; see part b of Figure 4. All the devices showed similar behavior with respect to their dopant concentrations, which suggests that the di-*tert*-butylphenylated indenofluorenyl moieties effectively prevent intermolecular interactions and concentration quenching.

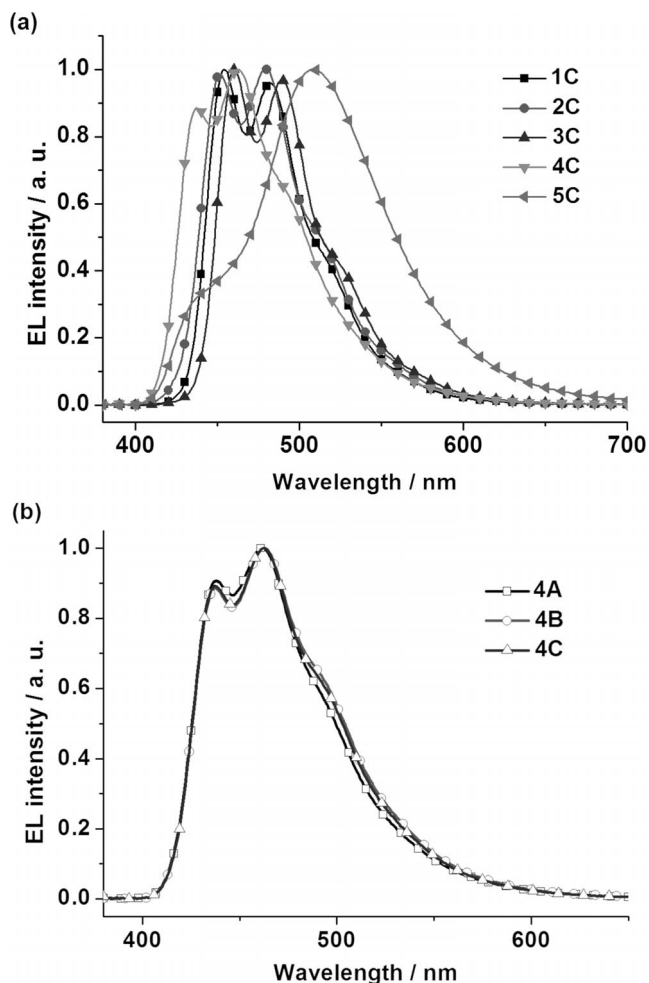


Figure 4. (a) EL spectra of blue-emitting devices **1C–5C**. (b) EL spectra of devices **4A–4C** at various doping concentration (3, 5, and 7%).

The current density–voltage–luminance (J – V – L) characteristics of devices **1A–1C** and the luminous efficiencies (LE), power efficiencies (PE), and external quantum efficiencies (EQE) of devices **1C–5C** with respect to current density are shown in Figure 5 and summarized in Table 2. All the devices showed low turn-on voltages of 3.5–5.0 V with stable blue emission from all over the surface. The devices with **1–3** showed higher turn-on voltages than those with **4** or **5**. The turn-on voltage was dependent on the charge-transport properties of the dopant and on the different levels of charge trapping by the HOMO and LUMO levels. The devices with **1–3** showed high EQEs (>5%) that nearly exceed the theoretical limits of fluorescent OLEDs. The high EQEs were attributed to the di-*tert*-butylphenylated indeno[1,2-*b*]fluorenyl cores with (diphenylamino)arylvinyl groups. The varying performances of the devices sug-

gest that structural variation of the dopants' spacer groups and positional changes in the indenofluorene cores greatly affect the performances of the solid-state devices. For example, changing the dopants' spacer groups from phenyl to fluorenyl moieties (**1** vs. **3**) increased the device's EQE by 25–56%. Devices containing **3** showed the highest EQEs.

Devices with **2**, containing biphenyl moieties as the spacer groups, showed EQEs reduced by 6–14% relative to those with **1** with phenyl spacer groups. Device **3A** with fluorenyl spacer units showed the best luminance of the devices with indenofluorene core groups. The best luminous efficiency of 12.2 cd A⁻¹, power efficiency of 6.08 lm W⁻¹, and

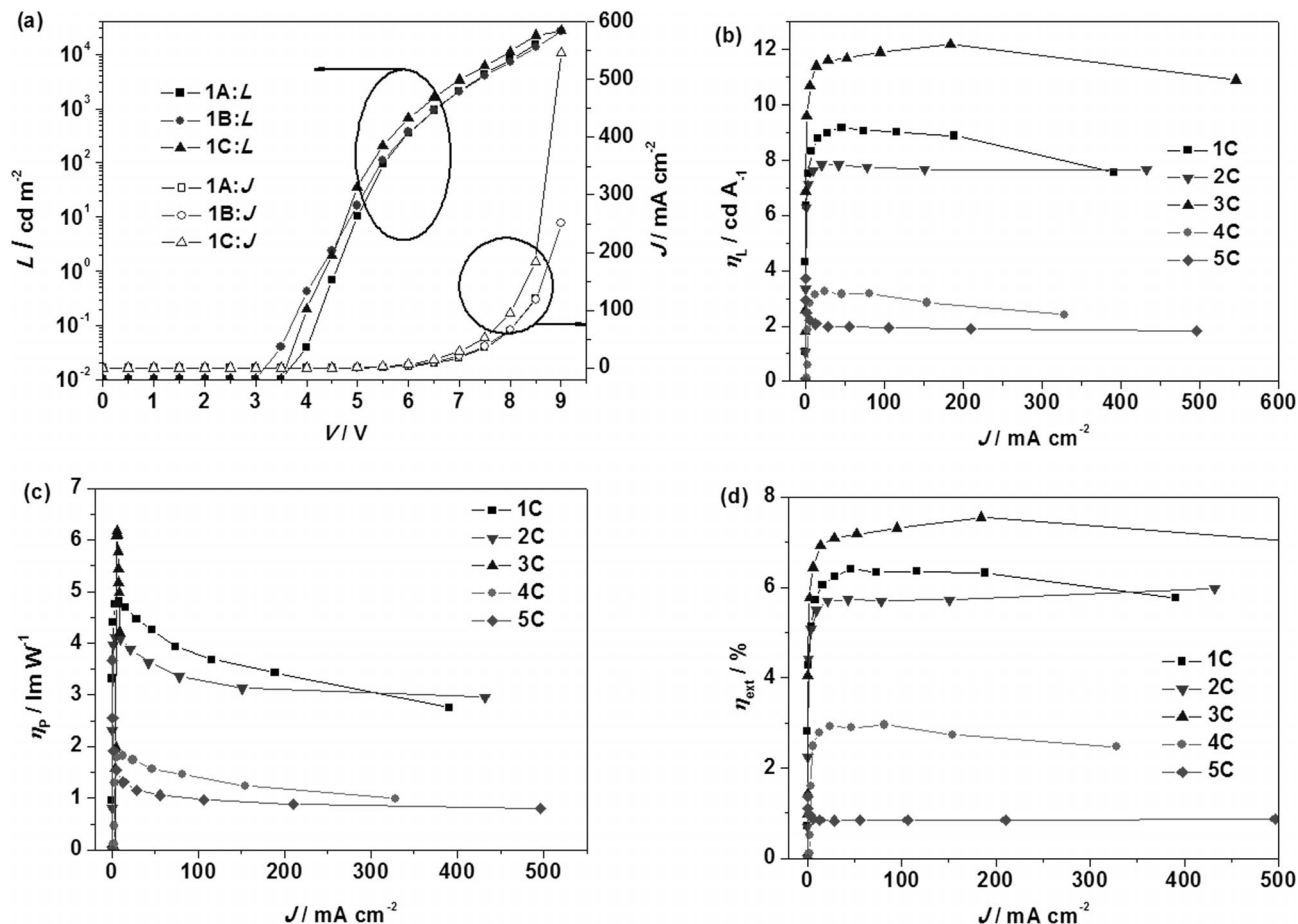


Figure 5. (a) J - V - L data for devices **1A**–**1C**. (b) Luminous efficiencies, (c) power efficiencies, and (d) external quantum efficiencies of the devices **1C**–**5C** as a function of current density.

Table 2. EL performance characteristics of devices **1**–**5**.

Device	Doping [%]	V_{on} [V]	EL _{max} [nm]	L [cd/m ²] ^[a]	LE [cd/A] ^[b,c]	PE [lm/W] ^[b,c]	EQE [%] ^[b,c]	CIE (x , y) ^[d]
1A	1 (3)	4.5	453/481	10740	8.06/7.81	4.41/4.10	5.96/5.70	(0.145, 0.194)
1B	1 (5)	4.5	454/482	10260	8.44/8.22	4.62/4.31	6.17/6.00	(0.145, 0.198)
1C	1 (7)	4.5	455/483	10480	9.19/8.92	4.82/4.60	6.40/6.12	(0.146, 0.212)
2A	2 (3)	5.0	451/479	7541	7.00/7.00	3.98/3.47	5.34/5.28	(0.149, 0.183)
2B	2 (5)	5.0	451/474	7863	7.84/7.72	4.11/3.83	5.73/5.55	(0.150, 0.194)
2C	2 (7)	5.0	452/480	11580	7.84/7.84	4.12/3.89	5.98/5.69	(0.149, 0.193)
3A	3 (3)	5.0	459/488	15290	12.6/12.2	6.69/6.08	8.21/7.84	(0.148, 0.241)
3B	3 (5)	4.5	460/489	13420	11.3/11.1	5.04/5.04	7.14/6.30	(0.149, 0.250)
3C	3 (7)	4.5	461/491	22410	12.2/11.5	6.18/5.95	7.55/7.01	(0.151, 0.257)
4A	4 (3)	4.0	438/461	8767	2.98/2.97	2.13/1.59	2.87/2.81	(0.153, 0.121)
4B	4 (5)	4.0	437/463	8887	3.13/3.07	1.77/1.70	2.82/2.69	(0.153, 0.133)
4C	4 (7)	4.0	437/462	7952	3.25/3.25	1.82/1.74	2.96/2.93	(0.153, 0.128)
5A	5 (3)	4.0	507	7394	2.21/2.21	1.59/1.28	0.91/0.91	(0.222, 0.376)
5B	5 (5)	3.5	508	9490	1.99/1.90	1.18/1.12	0.89/0.81	(0.217, 0.362)
5C	5 (7)	3.5	507	9114	3.68/1.99	3.71/1.15	1.37/0.84	(0.216, 0.355)
MADN only		4.0	442	954	1.4/1.1	1.0/0.5	1.6/1.5	(0.15, 0.08)

[a] Maximum luminance 8.5 V. [b] Maximum values. [c] At 20 mA/cm². [d] Commission Internationale d'Éclairage (CIE) coordinates at 8.5 V.

the highest EQE of 7.84% at 20 mA cm⁻² were obtained with device 3A. Devices with dopant 3 showed more effective energy transfer from the MADN host to the dopant than devices with 1, 2, 4, and 5 due to the good spectral overlap between the emission of the MADN host and the dopant's absorption; see Figure 1 (a). Dopant 3 also exhibited the highest fluorescent emission quantum yield (0.97). These factors likely contributed to the improved EL efficiencies of the devices fabricated with 3. The low quantum yield of compound 5 (0.25) and the poor overlap of its absorption spectrum with the emission spectrum of the MADN host likely contributes to the reduced EL efficiencies of devices 5A–5C. These results suggest that effective Förster energy transfer between the host and dopant and the high fluorescent emission quantum yields of the dopants lead to highly efficient blue OLEDs. The EL efficiencies of the devices were not significantly reduced by increasing the doping to 7%. These observations indicate that tetraethylated indenofluorene derivatives containing a (diphenylamino)arylvinyl group and di-*tert*-butylphenyl blocking units reduce molecular aggregation in the emitting layer, preventing concentration quenching.

Conclusions

Blue fluorescent indenofluorene derivatives containing (diphenylamino)arylvinyl groups and di-*tert*-butylphenyl blocking units exhibit high EL performances. The device with 3% of 3 as blue dopant shows a luminous efficiency of 12.2 cd A⁻¹, a power efficiency of 6.08 lm W⁻¹, and an external quantum efficiency of 7.84% at 20 mA cm⁻¹. Its CIE coordinates are (0.148, 0.241) at 8.5 V. A deep-blue OLED with CIE coordinates (0.153, 0.128) at 8.5 V was prepared by using compound 4 as the dopant. It exhibits a luminous efficiency of 3.25 cd A⁻¹, a power efficiency of 1.74 lm W⁻¹, and an external quantum efficiency of 2.93% at 20 mA cm⁻¹. Di-*tert*-butylphenylated indeno[1,2-*b*]fluorenyl derivatives were shown to possess properties suitable for use in blue-emitting OLEDs.

Experimental Section

General Methods: ¹H and ¹³C NMR spectra were recorded in CDCl₃ with a Varian spectrometer (Unity Inova 300Nb or Unity Inova 500Nb). FTIR spectra were recorded with a Bruker VERTEX70 or TENSOR27 spectrometer. Low- and high-resolution mass spectra were measured by using a JEOL JMS-AX505WA spectrometer in FAB mode. UV/Vis absorption spectra of the blue-emitting compounds in dichloromethane (10⁻⁵ M) in quartz cuvettes (1.0 cm paths) were acquired by using a Sinco S-3100 spectrophotometer at 293 K. Photoluminescence spectra were measured with an Amincobrowman series 2 luminescence spectrometer. Fluorescence quantum yields were determined in nitrogen-degassed dichloromethane at 293 K against a BDAVBi reference ($\Phi = 0.86$)^[20] and as films formed on quartz plates (50 nm) using BDAVBi as a standard ($\Phi_f = 30\%$ measured by the calibrated integration sphere system).^[21] HOMO energies were determined by using a low-energy photoelectron spectrometer (Riken-Keiki, AC-2). Bandgap energies

were determined from the intersections of the absorption and photoluminescence spectra. LUMO energies were calculated by subtracting the corresponding optical bandgap energies from the HOMO values.

Materials and Syntheses: Solvents for organic synthesis were reagent- or HPLC-grade. Only HPLC-grade solvents were used in photophysical spectroscopy and fluorescence quantum yield measurements. THF was dried with sodium benzophenone ketyl anion radicals and distilled under a dry nitrogen immediately prior to use. Commercially available reagents were used without further purification unless otherwise stated. Diethyl 4-(diphenylamino)benzylphosphonate (6),^[22] diethyl [4'-(diphenylamino)biphenyl-4-yl]methylphosphonate (7),^[23] diethyl (7-diphenylamino-9,9-diethylfluorene-2-yl)methylphosphonate (8),^[24] diethyl [9-(3,5-di-*tert*-butylphenyl)-9*H*-carbazolyl]methylphosphonate (9),^[25] 2,8-dibromo-6,6,12,12-tetraethylindeno[1,2-*b*]fluorene (10),^[15] and 1,3-dihydroindeno[2,1-*b*]fluorene (13)^[18] were prepared as reported elsewhere.

General Procedure for the Horner–Wadsworth–Emmons Reactions: Potassium *tert*-butoxide (2.3 mmol) was added to a solution of 2-(3,5-di-*tert*-butylphenyl)-8-formyl-6,6,12,12-tetraethylindeno[1,2-*b*]fluorene (1.5 mmol) and the corresponding phosphonate (1.5 mmol) in THF in an ice bath under nitrogen. The reaction mixture was stirred for 15 min at 0 °C for 1 h at room temperature and then quenched with water. The mixture was extracted with ethyl acetate and washed twice with water. The combined organic layers were dried with MgSO₄ and the solvent was removed under reduced pressure to afford a crude product that was purified by silica gel column chromatography and subsequent recrystallization from CH₂Cl₂/EtOH.

Device Fabrication and Measurement: The blue devices had configurations of indium tin oxide (ITO, 150 nm)/*N,N'*-diphenyl-*N,N'*-bis[4-(phenyl-*m*-tolylamino)phenyl]biphenyl-4,4'-diamine (DNTPD, 60 nm)/*N,N'*-bis(1-naphthyl)-*N,N'*-diphenylbenzidine (NPB, 30 nm)/MADN:dopants (30 nm)/tris(8-hydroxyquinolinyl)aluminum (Alq₃, 20 nm)/LiF (1.0 nm)/Al (200 nm). All organic compounds, except the dopants, were deposited at 1 Å/s. Device current (*J*)–voltage (*V*)–luminance (*L*) characteristics and electroluminescence (EL) spectra were measured by using a Keithley 2400 measurement unit and CS 1000A spectrophotometer, respectively.

Supporting Information (see footnote on the first page of this article): Detailed experimental procedures, characterization data, ¹H and ¹³C NMR spectra for all new compounds, low-energy photoelectron spectra of compounds 1–5.

Acknowledgments

This research was supported by the Korean Ministry of Education, Science and Technology, National Research Foundation (NRF) (Basic Science Research Program) (20110004655). J. Y. L. acknowledges financial support from the Gyeonggi Province (GRRC program Dankook2011-B01: Materials Development for High-Efficiency Solid-State Lighting) and from the Development of Core Technologies for Organic Materials Applicable to OLED Lighting with High Color Rendering Index by the Ministry of Knowledge and Economy (MKE).

- [1] H. Sirringhaus, N. Tessler, R. H. Friend, *Science* **1998**, *280*, 1741–1744.
- [2] C. T. Chen, Y. Wei, J. S. Lin, M. V. R. K. Moturu, W. S. Chao, Y. T. Tao, C. H. Chien, *J. Am. Chem. Soc.* **2006**, *128*, 10992–10993.

- [3] Z.-Y. Xia, Z.-Y. Zhang, J.-H. Su, Q. Zhang, K.-M. Fung, M.-K. Lam, K.-F. Li, W.-Y. Wong, K.-W. Cheah, H. Tian, C. H. Chen, *J. Mater. Chem.* **2010**, *20*, 3768–3774.
- [4] J. Huang, J.-H. Su, X. Li, M.-K. Lam, K.-M. Fung, H.-H. Fan, K.-W. Cheah, C. H. Chen, H. Tian, *J. Mater. Chem.* **2011**, *21*, 2957–2964.
- [5] K. T. Wong, T. Y. Hwu, A. Balaiah, T. C. Chao, F. C. Fang, C. T. Lee, Y. C. Peng, *Org. Lett.* **2006**, *8*, 1415–1418.
- [6] C. C. Wu, Y. T. Lin, K. T. Wong, R. T. Chen, Y. Y. Chien, *Adv. Mater.* **2004**, *16*, 61–65.
- [7] J. Luo, Y. Zhou, Z. Q. Niu, Q. F. Zhou, Y. G. Ma, J. Pei, *J. Am. Chem. Soc.* **2007**, *129*, 11314–11315.
- [8] A. C. Chen, S. W. Gulligan, Y. Geng, S. H. Chen, K. P. Klubek, K. M. Vaeth, C. W. Tang, *Adv. Mater.* **2004**, *16*, 783–788.
- [9] C.-F. Shu, R. Dodda, F.-I. Wu, M. S. Liu, A. K.-Y. Jen, *Macromolecules* **2003**, *36*, 6698–6703.
- [10] N. Matsumoto, T. Miyazaki, M. Nishiyama, C. Adachi, *J. Phys. Chem. C* **2009**, *113*, 6261–6266.
- [11] S. Merlet, M. Birau, Z. Y. Wang, *Org. Lett.* **2002**, *4*, 2157–2159.
- [12] C. Poriel, J.-J. Liang, J. Rault-Berthelot, F. Barriere, N. Cocherel, A. M. Z. Slawin, D. Horhant, M. Virboul, G. Alcaraz, N. Audebrand, L. Vignau, N. Huby, G. Wantz, L. Hirsch, *Chem. Eur. J.* **2007**, *13*, 10055–10069.
- [13] T. Hadizad, J. Zhang, Z. Y. Wang, T. C. Gorjanc, C. Py, *Org. Lett.* **2005**, *7*, 795–797.
- [14] D. Marsitzky, J. C. Scott, J. P. Chen, V. Y. Lee, R. D. Miller, S. Setayesh, K. Muellen, *Adv. Mater.* **2001**, *13*, 1096–1099.
- [15] Y. Park, J.-H. Lee, D. H. Jung, S.-H. Liu, Y.-H. Lin, L.-Y. Chen, C.-C. Wu, J. Park, *J. Mater. Chem.* **2010**, *20*, 5930–5936.
- [16] C. Poriel, R. Métivier, J. R. Berthelot, D. Thirion, F. Barrière, O. Jeannin, *Chem. Commun.* **2011**, *47*, 11703–11705.
- [17] F. Ebel, W. Deutschel, *Ber. Dtsch. Chem. Ges.* **1956**, *89*, 2794–2799.
- [18] H. N. Shin, C. S. Kim, Y. J. Cho, H. J. Kwon, B. O. Kim, S. M. Lim, S. S. Yoon (Dow Advanced Displays Materials), PCT Int. Appl., WO 2010114243, **2010**.
- [19] M. J. Frisch, G. W. Trucks, H. B. Schlegel, G. E. Scuseria, M. A. Robb, J. R. Cheeseman, J. A. Montgomery, T. Vreven Jr., K. N. Kudin, J. C. Burant, J. M. Millam, S. S. Iyengar, J. Tomasi, V. Barone, B. Mennucci, M. Cossi, G. Scalmani, N. Rega, G. A. Petersson, H. Nakatsuji, M. Hada, M. Ehara, K. Toyota, R. Fukuda, J. Hasegawa, M. Ishida, T. Nakajima, Y. Honda, O. Kitao, H. Nakai, M. Klene, X. Li, J. E. Knox, H. P. Hratchian, J. B. Cross, C. Adamo, J. Jaramillo, R. Gomperts, R. E. Stratmann, O. Yazyev, A. J. Austin, R. Cammi, C. Pomelli, J. W. Ochterski, P. Y. Ayala, K. Morokuma, G. A. Voth, P. Salvador, J. J. Dannenberg, V. G. Zakrzewski, S. Dapprich, A. D. Daniels, M. C. Strain, O. Farkas, D. K. Malick, A. D. Rabuck, K. Raghavachari, J. B. Foresman, J. V. Ortiz, Q. Cui, A. G. Baboul, S. Clifford, J. Cioslowski, B. B. Stefanov, G. Liu, A. Liashenko, P. Piskorz, I. Komaromi, R. L. Martin, D. J. Fox, T. Keith, M. A. Al-Laham, C. Y. Peng, A. Nanayakkara, M. Challacombe, P. M. W. Gill, B. Johnson, W. Chen, M. W. Wong, C. Gonzalez, J. A. Pople, *Gaussian 03*, rev. B05, Gaussian, Inc., Pittsburgh, PA, **2003**.
- [20] K. H. Lee, C. S. Son, J. Y. Lee, S. Kang, K. S. Yook, S. O. Jeon, J. Y. Lee, S. S. Yoon, *Eur. J. Org. Chem.* **2011**, 4788–4798.
- [21] J. C. de Mello, H. F. Wittmann, R. H. Friend, *Adv. Mater.* **1997**, *9*, 230–232.
- [22] S. Zheng, S. Barlow, T. C. Parker, S. R. Marder, *Tetrahedron Lett.* **2003**, *44*, 7989–7992.
- [23] K. H. Lee, S. O. Kim, J. N. You, S. Kang, J. Y. Lee, K. S. Yook, S. O. Jeon, J. Y. Lee, S. S. Yoon, *J. Mater. Chem.* **2012**, *22*, 5145–5154.
- [24] K. H. Lee, L. K. Kang, J. Y. Lee, S. Kang, S. O. Jeon, K. S. Yook, J. Y. Lee, S. S. Yoon, *Adv. Funct. Mater.* **2010**, *20*, 1345–1358.
- [25] K. H. Lee, S. O. Kim, K. S. Yook, S. O. Jeon, J. Y. Lee, S. S. Yoon, *Synth. Met.* **2011**, *161*, 2024–2030.

Received: February 1, 2012
Published Online: April 10, 2012